



UNIVERSIDAD CARLOS III DE MADRID

working
papers

Working Paper 14-26
Statistics and Econometrics Series 18
October 2014

Departamento de Estadística
Universidad Carlos III de Madrid
Calle Madrid, 126
28903 Getafe (Spain)
Fax (34) 91 624-98-48

Score Driven Asymmetric Stochastic Volatility Models

Xiuping Mao^a, Esther Ruiz^{a,b*}, Helena Veiga^{a,b,c}

Abstract

In this paper we propose a new class of asymmetric stochastic volatility (SV) models, which specifies the volatility as a function of the score of the distribution of returns conditional on volatilities based on the Generalized Autoregressive Score (GAS) model. Different specifications of the log-volatility are obtained by assuming different return error distributions. In particular, we consider three of the most popular distributions, namely, the Normal, Student-t and Generalized Error Distribution and derive the statistical properties of each of the corresponding score driven SV models. We show that some of the parameters cannot be properly identified by the moments usually considered as to describe the stylized facts of financial returns, namely, excess kurtosis, autocorrelations of squares and cross-correlations between returns and future squared returns. The parameters of some restricted score driven SV models can be estimated adequately using a MCMC procedure. Finally, the new proposed models are fitted to financial returns and evaluated in terms of their in-sample and out-of-sample performance.

Keywords: BUGS, Generalized Asymmetric Stochastic Volatility, Leverage effect, MCMC, Score driven models

^aDepartament of Statistics, Universidad Carlos III de Madrid.

^bInstituto Flores de Lemus, Universidad Carlos III de Madrid.

^cFinancial Research Center/UNIDE, Avenida das Forças Armadas, 1600-083, Lisboa, Portugal.

*C/ Madrid, 126, 28903, Getafe, Madrid (Spain), Tel: +34 916249851, Fax: +34 916249848, Email: ortega@est-econ.uc3m.es. *Corresponding Author*.

Acknowledgments: Financial support from the Spanish Ministry of Education and Science, research project ECO2012-32401, is acknowledged. The third author is also grateful for project MTM2010-17323.

Score Driven Asymmetric Stochastic Volatility Models *

Xiuping Mao^a, Esther Ruiz^{•,h,•}, Helena Veiga^{•,b,c}

^aDepartment of Statistics, Universidad Carlos III de Madrid.

^bInstituto Flores de Lemus, Universidad Carlos III de Madrid.

^cFinancial Research CenterfUNIDE, Avenida das Forças Armadas, 1600-083, Lisboa, Portugal.

Abstract

In this paper we propose a new class of asymmetric stochastic volatility (SV) models, which specifies the volatility as a function of the score of the distribution of returns conditional on volatilities based on the Generalized Autoregressive Score (GAS) model. Different specifications of the log-volatility are obtained by assuming different return error distributions. In particular, we consider three of the most popular distributions, namely, the Normal, Student-t and Generalized Error Distribution and derive the statistical properties of each of the corresponding score driven SV models. We show that some of the parameters cannot be properly identified by the moments usually considered as to describe the stylized facts of financial returns, namely, excess kurtosis, autocorrelations of squares and cross-correlations between returns and future squared returns. The parameters of some restricted score driven SV models can be estimated adequately using a MCMC procedure. Finally, the new proposed models are fitted to financial returns and evaluated in terms of their in-sample and out-of-sample performance.

Keywords: BUGS, Generalized Asymmetric Stochastic Volatility, Leverage effect, MCMC, Score driven models

JEL: C22

*Financial support from the Spanish Ministry of Education and Science, research project EC02012-32401, is acknowledged. The third author is *also* grateful for project MTM2010-17323.

[•]*ej* Madrid, 126, 28903, Getafe, Madrid (Spain), Tel: +34 916249851, Fax: +34 916249849, Email: ortega@est-econ.uc3m.es. Corresponding Author.

1. Introduction

There is a large literature on modelling the second order dynamics of univariate financial returns with leverage effect. The main interest is to obtain accurate volatility estimates which are important components of many financial models. Two main alternative families of models are usually implemented to represent the dynamic evolution of asymmetric volatilities. The first family is based on the Generalised Autoregressive Conditional Heteroscedasticity (GARCH) model of [Bollerslev \(1986\)](#), with the volatility specified as a function of past returns and, consequently, observable one-step ahead; see [Engle \(1995\)](#), [Giraitis et al. \(2007\)](#) and [Terasvirta \(2009\)](#) for comprehensive reviews on GARCH models and [Rodríguez and Ruiz \(2012\)](#) for a review on popular GARCH models with leverage effect. Alternatively, the second family includes Stochastic Volatility (SV) models, which specify the volatility as a latent variable that is not directly observable; see [Ghysels et al. \(1996\)](#) and [Cavaliere \(2006\)](#) for reviews on SV models and their applications and [Mao et al. \(2013\)](#) for the comparison of popular alternative asymmetric SV models.

Besides heteroscedasticity and leverage effect, another important and well documented empirical feature of standardized financial returns is the fact that they are heavy-tailed distributed; see, for instance, [Liesenfeld and Jung \(2000\)](#), [Jacquier et al. \(2004\)](#) and [Chen et al. \(2008\)](#) among many others. In order to capture this latter feature, both GARCH and SV models have been extended by assuming fat-tailed return errors. Two examples are the GARCH-t model of [Bollerslev \(1987\)](#) and the asymmetric SV model with Student-t distribution of [Asai and McAleer \(2011\)](#). Nonetheless, these traditional models often specify the asymmetric volatility as being driven by past return errors. Consequently, they can suffer from a potential drawback since a large realisation of the return error, which could be due to the heavy-tailed nature of its distribution, will be attributed to an increase in volatility. Therefore, in the GARCH

context, [Creal et al. \(2013\)](#) and [Harvey \(2013\)](#) have recently proposed models in which the dynamic of volatility is driven by the lagged score of the conditional distribution of returns to automatically correct for influential observations. This gives rise to the Generalised Autoregressive Score (GAS) models which are also known as dynamic conditional score (DOS) models.

In this paper, we extend the GAS idea to SV models by specifying the unobserved volatility to be driven by lagged scores. Given that the conditional distribution of returns does not have an analytical expression, the score is computed with respect to the distribution of returns conditional on the volatilities. We show that this type of models lay in the Generalised Asymmetric SV (GASV) family recently proposed by [Mao et al. \(2013\)](#). We denote the new models as GAS-GASV (GAS^2V) and consider three alternative GAS^2V models depending on the assumed distribution of the return errors, namely, Normal, Student-t and Generalised Error Distribution (GED). Closed-form expressions of several relevant statistics of these models are derived to analyse their ability to represent the main empirical features often observed in financial returns, namely, the excess kurtosis, positive autocorrelations of power-transformed absolute returns and negative cross-correlations between returns and future power-transformed absolute returns. It is important to point out that analytical expressions of these moments of the GAS^2V model with Student-t errors can now be derived, in opposition to the traditional specifications of the SV models in which their derivation is hardly possible when the errors are Student-t. Moreover, we show that the GAS^2V model with Student-t errors generates returns with very similar properties as those generated by the GAS^2V model with GED errors as far as the parameters of both distributions are chosen to have the same kurtosis. Therefore, there could be difficulties in identifying the parameters of the GAS^2V model when looking at the moments.

Although SV models are considered competitive alternatives to GARCH models,

their estimation usually limits their empirical implementation due to the intractability of their likelihood function; see [Carnero et al. \(2004\)](#) for the advantages of SV models when compared with GARCH models. In recent decades, many efforts have been done in this direction and considerable advances have been achieved with simulation based procedures being a very popular alternatives; see [Broto and Ruiz \(2004\)](#) for a survey on the estimation of SV models. Examples of procedures based on the Monte Carlo likelihood evaluation are the simulated Maximum Likelihood (MCL) procedure of [Durbin and Koopman \(1997\)](#) and the Efficient Importance Sampling (EIS) procedure of [Liesenfeld and Richard \(2003\)](#) and [Richard and Zhang \(2007\)](#); see also [Asai and McAleer \(2011\)](#) for the implementation of the latter procedure for estimating their exponential SV model and [Koopman et al. \(2014\)](#) for an extension. Alternatively, Monte Carlo Markov Chain (MCMC) has become a standard estimation method because it is efficient without relying on asymptotic approximations for inference on the parameters; see, for example, [Jacquier et al. \(1994\)](#), [Omori et al. \(2007\)](#), [Abanto-Valle et al. \(2010\)](#), [Tsiotas \(2012\)](#) and [Yu \(2005, 2012\)](#) among others for implementations of MCMC to estimate SV models. Furthermore, MCMC also allows obtaining one-step-ahead densities of the underlying volatilities. In this paper, we consider a MCMC estimator implemented by the user-friendly and freely available software BUGS; see [Meyer and Yu \(2000\)](#) and [Yu \(2005, 2012\)](#) for the reliability of BUGS when estimating the parameters of the SV model. We conduct an intensive Monte Carlo study on the finite sample properties of the MCMC estimator implemented using BUGS when estimating the model parameters and find that it is adequate when the model is restricted as to avoid the identification issues detected when looking at the statistical properties of the GAS²V models. Using the MCMC estimator, the three GAS²V models considered in this paper are fitted to a series of daily S&P500 returns and two series of weekly financial returns, namely S&P500 and NIKKEI225. The performance is evaluated both in-sample and out-of sample.

The remainder of this paper is organized as follows. In [section 2](#), the GAS²V model is proposed and its statistical properties are derived when the errors are Gaussian, Student-t and GED. In [section 3](#), we perform a Monte Carlo experiment to analyse the finite sample properties of the MCMC estimator of the model parameters. The GAS²V models are fitted to daily and weekly real time series of financial returns and their in-sample and out-of-sample performances are evaluated in [section 4](#). Finally, we conclude in [section 5](#).

2. Score driven asymmetric SV models

In this section, we propose the GAS²V model and derive its statistical properties when the errors have Normal, Student-t and GED distribution. In particular, we obtain closed-form expressions of the marginal variance, the kurtosis, the autocorrelation function (acf) of power-transformed absolute returns and cross-correlation function (ccf) between returns and future power-transformed absolute returns.

2.1. The GAS²V model

Let Y_t be the return at time t , h_t its volatility and $h_t = \log \sigma_t^2$. The family of GAS²V models is defined as follows¹

$$y_t = \exp(h_t/2)\epsilon_t, \quad t = 1, 2, \dots, T, \quad (1)$$

$$h_{t-p} = \langle P(h_{t-1-p}) + f(U_{t-1}) + \gamma T_{jt-1}, \quad (2)$$

where T_{jt} is a Gaussian white noise with variance γ and ϵ_t is a strict white noise with variance one which is distributed independently of T_{jt} for all leads and lags. p is a scale parameter related with the marginal variance of returns while the parameter $\langle P$

¹We only consider one lag of past scores and volatilities as this is the most popular specification in the empirical implementation of related similar models for volatilities.

is related with the persistence of the volatility shocks. Finally, $f(\cdot)$ is a function of the scaled conditional score of the lagged return, U_{t-1} , which is defined as follows

$$u_t = C \frac{\partial \ln P(y_t | h_t)}{\partial h_t}, \quad (3)$$

where C is any real number introduced to simplify the expression of the score and $P(Y_t | h_t)$ is the density of returns conditional on volatilities. Denoting by $1/(E_t)$ the probability density function (pdf) of h_t , the density function of Y_t conditional on h_t is given by $P(y_t | h_t) = \exp(-h_t/2) 1/J(Y_t \exp(-h_t/2))$. It follows immediately that

$$u_t = -\frac{C}{2} + \frac{C}{2} \frac{\epsilon_t \psi'(\epsilon_t)}{\psi(\epsilon_t)}, \quad (4)$$

where $1/J(E_t)$ denotes the derivative of $1/(E_t)$ with respect to h_t . Thus, U_t depends on E_t and, consequently, after writing $f(U_{t-d} = f(-\mathbf{1} + \mathbf{1}E_t \mathbf{1} E))$ in equation (2), the GAS²V model in equations (1) and (2) can be obtained as a particular case of the GASV family defined by [Mao et al. \(2013\)](#) and the results on the properties of this family can be directly used. In particular, according to Theorem 2.1 of [Mao et al. \(2013\)](#), when $\lim_{t \rightarrow \infty} \phi^t < 1$ and the distribution of E_t is such that $E(\exp(f(E_t))) < \infty$, the GAS²V model is stationary. Moreover, for any non-negative integer e , if the distribution of E_t is such that $E(\exp(0.5cf(E_t))) < \infty$ and $E(\mathbf{1}E_t\mathbf{1}c) < \infty$, both Y_t and $\mathbf{1}Y_t\mathbf{1}$ have finite moments of order c . In particular, the marginal variance and kurtosis of Y_t are given by

$$\sigma_y^2 = \exp\left(\mu + \frac{\sigma_\eta^2}{2(1-\phi^2)}\right) P(\phi^{i-1}) \quad (5)$$

and

$$\kappa_y = \kappa_\epsilon \exp\left(\frac{\sigma_\eta^2}{1-\phi^2}\right) \frac{P(2\phi^{i-1})}{(P(\phi^{i-1}))^2}, \quad (6)$$

respectively, where $P(bi) = \prod_{i=1}^n E(\exp(bd(ut-i)))$.

Under the same conditions, Theorem 2.2 of [Mao et al. \(2013\)](#) established that the autocorrelation function of Y_t is also finite and given by

$$\rho_c(\tau) = \frac{E(|\epsilon_t|^c)E(|\epsilon_t|^c \exp(0.5c\phi^{\tau-1}f(\epsilon_t))) \exp\left(\frac{\phi^\tau c^2 \sigma_\eta^2}{4(1-\phi^2)}\right) P(0.5c(1+\phi^\tau)\phi^{i-1})T(\tau, 0.5c\phi^{i-1}) - [E(|\epsilon_t|^c)P(0.5c\phi^{i-1})]^2}{E(|\epsilon_t|^{2c}) \exp\left(\frac{c^2 \sigma_\eta^2}{4(1-\phi^2)}\right) P(c\phi^{i-1}) - [E(|\epsilon_t|^c)P(0.5c\phi^{i-1})]^2},$$

where $T(n, bt) = \prod_{i=1}^{n-1} E(\exp(bd(ut-i)))$ if $n > 1$ and $T(1, bi) = 1$. Finally, the finiteness of the cross-correlation function between Y_t and $Y_{t+\tau}$, for $\tau = 1, 2, \dots$, is guaranteed when further $E(|\epsilon_t|^{2c}) < \infty$. It is given by

$$\rho_{c1}(\tau) = \frac{E(|\epsilon_t|^c) \exp\left(\frac{c^2 \sigma_\eta^2}{4(1-\phi^2)}\right) E(\exp(0.5c\phi^{\tau-1}f(\epsilon_t))) P(0.5c(1+\phi^\tau)\phi^{i-1}) T(\tau, 0.5c\phi^{i-1}) - [E(|\epsilon_t|^c)P(0.5c\phi^{i-1})]^2}{E(|\epsilon_t|^{2c}) \exp\left(\frac{c^2 \sigma_\eta^2}{4(1-\phi^2)}\right) P(c\phi^{i-1}) - [E(|\epsilon_t|^c)P(0.5c\phi^{i-1})]^2}$$

Later in this paper, we obtain closed-form expressions of these moments for particular assumptions on the function $f(\cdot)$ and on the error distribution. In particular, in order to represent the leverage effect often observed when dealing with time series of financial returns, we consider the following specification $off(\cdot)$

$$f(U_{t-1}) = ct!(Et-1 < 0) + kut-1 + k^* \text{sign}(-Et-1)(ut-1 + 1), \quad (7)$$

where $I(\cdot)$ is an indicator function that takes value one when the argument is true and zero otherwise. The parameter k represents an ARCH effect while the parameters a and k^* represent the leverage effect with a dealing with changes in the scale parameter depending on the sign of past returns and k^* with changes in the dynamics involving the score. Note that the last term in (7) is based on the proposal of [Harvey \(2013\)](#) in the context of asymmetric score GARCH models. As pointed out by [Harvey \(2013\)](#), although the statistical validity of the model does not require it, proper restriction

may be imposed on k and k^* in order to ensure that an increase in the absolute value of a standardized observation does not lead to a decrease in volatility.

In order to represent the leverage effect, besides the cross-correlations, [Mao et al. \(2013\)](#) propose the Stochastic News Impact Surface (SNIS) that relates α_t with ϵ_{t-1} and η_{t-1} . As in [Engle and Ng \(1993\)](#), the lagged volatilities are evaluated at the marginal variance, so that, at time $t-1$, the volatility is equal to an "average" volatility. Consequently, the effect of level shocks, ϵ_{t-1} and volatility shocks, η_{t-1} on the volatility at time t is given by

$$SNIS_t = \exp((1 - \phi)\mu)\sigma_y^{2\phi} \exp(f(u_{t-1}) + \eta_{t-1}), \quad (8)$$

where α is the marginal variance of Y_t in (5) and $f(u_{t-1})$ is given in (7). It is important to note that the score, u_t , is different depending on the particular assumption on the error distribution. Several distributions of return errors have been proposed in the related literature being the Gaussian distribution the most popular; see, for example, [Jacquier et al. \(1994\)](#) and [Harvey and Shephard \(1996\)](#). When the errors are Gaussian, the score is given by

$$u_{t-1} = \epsilon_{t-1} - \alpha_{t-1}. \quad (9)$$

The corresponding SNIS is plotted in the top panel of [Figure 1](#) when the GAS²V model has parameters $\{\alpha, \phi, k^*, k, a\} = \{0.07, 0.98, 0.08, 0.1, 0.05\}$. The scale parameter, j , is chosen so that $\exp((1 - \phi)\mu)\sigma_y^{2\phi} = 1$. It shows that the volatility response is larger when the lagged return is negative than when it is positive. Therefore, this model is able to capture the leverage effect. Moreover, the difference in the response of the volatility to positive and negative ϵ_{t-1} depends on the log-volatility noise, η_{t-1} . Stronger leverage effect is observed when η_{t-1} is positive and large. The News Impact

Curve (NIC), defined by Engle and Ng (1993), is obtained when $\gamma_{t-1} = 0$, which is also plotted in Figure 1. The inclusion of γ_{t-1} in the model allows it to be more flexible in representing the leverage effect.

However, the Gaussian distribution does not fully capture the fat tails of financial time series often observed in practice and may suffer from a lack of robustness in the presence of extreme outlying observations. Consequently, several authors consider heavy-tailed distributions such as the Student-t or the GED distributions;² see, for example, Chen et al. (2008), Choy et al. (2008) and Wang et al. (2011, 2013). Consider first the GAS²V model when ϵ_t has a Student-t distribution with ν degrees of freedom. In this case, the score is given by

$$u_t = (\nu + 1) \frac{\epsilon_t^2}{\nu - 2 + \epsilon_t^2} - 1. \quad (10)$$

The SNIS of the GAS²V model with Student-t errors is plotted in the middle panel of Figure 1 for the same parameters as above and $\nu = 6$. The asymmetric response of volatility to ϵ_{t-1} is similar to that of the GAS²V model with Gaussian errors.

Finally, when ϵ_t is assumed to follow a GED(ν) distribution, then the score function is given by

$$u_t = \frac{\nu}{2} \left| \frac{\epsilon_t}{\varphi} \right|^\nu - 1, \quad (11)$$

with $r.p = \gamma^2 - 2/\nu r(1/\nu)/r(3/\nu)$. The SNIS of the GAS²V model with GED errors when $\nu = 1.5$ is plotted in the bottom panel of Figure 1. The volatility responds asymmetrically to the positive and negative returns errors. However, no big difference can be observed among the SNISs of all the three GAS²V models.

²There are also proposals to include simultaneously leptokurtosis and skewness in the distribution of ϵ_t , such as the skewed-Normal and skew-Student-t in Nakajima and Omori (2012) and the asymmetric GED in Cappuccio et al. (2004). It is not straightforward to capture the moments of returns when the distribution of ϵ_t is asymmetric. Consequently, we leave this extension for future research and focus on symmetric distributions.

2.2. Different GAS²V models

In this subsection, we analyze the properties of three GAS²V models corresponding to three different return error distributions.

2.2.1. GAS²V-N

If ϵ_t follows a Gaussian distribution, then, the scaled score, U_t is given by expression (9) and the specification of the log-volatility with JO defined as in (7) reduces to

$$h_t - \mu = \phi(h_{t-1} - \mu) + \alpha I(\epsilon_{t-1} < 0) + k(\epsilon_{t-1}^2 - 1) + k^* \text{sign}(-\epsilon_{t-1}) \epsilon_{t-1}^2 + \eta_{t-1}. \quad (12)$$

The resulting model is denoted as GAS²V-N. It is important to note that although the specification of the volatility in (12) is closely related to that in the T-GASV model of [Mao et al. \(2013\)](#), the way in which the leverage is introduced is different in both cases. In (12), the log-volatility depends on squared returns and the leverage effect is introduced in the same fashion as in the TGARCH model of [Zakoian \(1994\)](#). However, the log-volatility in the T-GASV model depends on past absolute returns and the leverage is introduced as in the EGARCH model. [Rodríguez and Ruiz \(2012\)](#) show that the TGARCH and EGARCH models are very similar. Therefore, we expect that, if ϵ_t is Gaussian, the GAS²V-N and T-GASV models have very similar properties. The analytical expressions of $E(\exp(bf(t:t)))$ and $E(I_t \exp(bf(t:t)))$ are given in [Appendix A.1](#). Using these expressions we can verify that when $|k| < 1$ and $k + W < 1/2$, the model is stationary, Y_t and $|Y_t|$ have finite moments of order e and the acf of $|Y_t|$ and ccf between Y_t and $|Y_{t+h}|$ are finite when $ck + |k| < 1$.

We first explore the kurtosis of the GAS²V-N model. It is the kurtosis of the ARSV(1) model proposed by [Harvey et al. \(1994\)](#), $k \exp C \cdot j$, multiplying the factor $R = \frac{1}{1 - E(\epsilon_t^2)}$ as a function of the leverage parameters a and k^* when $k = 0$ and 0.1 for three different persistence

parameters, namely, $\lambda = 0.5, 0.9$ and 0.98 . For these particular parameter values, we can observe that the ratio is always larger than 1. Therefore, the GAS²V-N model generates returns with larger kurtosis than the corresponding basic ARSV(1). Furthermore, the kurtosis increases with α , k^* and k . The increment is more prominent when λ is larger.

In order to illustrate how the autocorrelations and the cross-correlations depend on the parameters, we have considered a particular GAS²V-N model with parameters $\lambda = 0.98$ and $\mu = 0.05$. The leverage parameters α and k^* take values between 0 and 0.2 and 0 and 0.1, respectively. Figure 3 plots the first order autocorrelations of squares, $\rho_2(1)$ (top left panel), the first order autocorrelations of absolute returns, $\rho_1(1)$ (top right panel), and the first order cross-correlations between returns and future squared returns, $\rho_{21}(1)$ (bottom left panel), and future absolute returns, $\rho_{11}(1)$ (bottom right panel) when $k = 0$. These moments are also plotted in Figure 4 when $k = 0.1$. We can observe that they have very similar patterns as those of the GASV model; see Figure 2 of Mao et al. (2013). First, the first order autocorrelations are positive and the surface is rather flat and it is not affected by the leverage effect parameters k^* and α . However, the first order autocorrelation of absolute returns is larger than that of the squared returns and increases with the two parameters. Finally, the cross-correlations are negative and decrease with the two leverage effect parameters, α and k^* linearly. By comparing Figure 3 and Figure 4, we can observe that larger value of k gives larger first order autocorrelations but negligible difference in cross-correlations.

To illustrate the shape of these moments for different lags, Figure 5 plots the first twenty orders of these moments for a GAS²V-N model with parameters $\lambda = 0.98$, $\mu = 0.05$, $\alpha = 0.07$, $k^* = 0.1$ when $k = 0$, while Figure 6 illustrates these moments when $k = 0.1$. The values of the parameters are chosen to be very

similar to those obtained when fitting these models to financial data; see [section 4](#). The figures show that both the acf and absolute ccf decay exponentially towards zero. The absolute values of the moments related with absolute returns are larger than those of the squared returns. Therefore, we can conclude that the model is able to capture the Taylor Effect, phenomenon characterised by the autocorrelations of absolute returns to be larger than those of squares. Moreover, the larger value of k allows the model to capture larger autocorrelations of squared and absolute returns, therefore, volatility clustering.

2.2.2. GAS²V-T

Alternatively, if f_t is distributed as a standardized Student-t distribution with degrees of freedom $\nu_0 > 2$, pdf $f(f_t) = \frac{\Gamma(\frac{\nu_0+1}{2})}{\Gamma(\frac{\nu_0}{2})} \frac{1}{\sqrt{\nu_0}} (1 + \frac{f_t^2}{\nu_0})^{-\frac{\nu_0+1}{2}}$ with $\nu_0 =$

then U_t is given by (10). We denote the model specified by equations (1), (2), (7) and (10) as GAS²V-T. When $\nu_0 > 1$, the model is stationary. Moreover, for some non-negative integer e , if $\nu_0 > e$, then the acf of $|Y_t|^e$ is finite. If further, $\nu_0 > 2c$, the ccf between Y_t and $|Y_{t+\tau}|^c$ for a positive integer τ is also finite. The expectations needed to obtain the analytical expressions of the moments are derived in [Appendix A.2](#).

Analogously, we illustrate the kurtosis of GAS²V-T by plotting the factor R in [Figure 2](#), for the same parameters chosen for the GAS²V-N model and $\nu_0 = 11.8745$. Note that ν_0 guarantees ϵ_t to have the same kurtosis when it follows a GED distribution with degrees of freedom $\nu = 1.5$. We can observe that the ratio of the GAS²V-T model is smaller than that of the GAS²V-N when $c > 0.98$, while they are indistinguishable when c is small.

As previously, we illustrate the first order of the acfs and ccfs of GAS²V-T models in [Figure 3](#) and [Figure 4](#) when $\nu_0 = 11.8745$. The other parameters are the same

as those chosen for the GAS²V-N model. We observe that the GAS²V-N model generates larger first order autocorrelations for both absolute and squared returns than the corresponding GAS²V-T models. Moreover, the absolute values of the cross-correlations are also larger for the GAS²V-N model than for the GAS²V-T when $k = 0$. However, the absolute cross-correlation between returns and future squared returns are smaller in the case of the GAS²V-N when $k = 0.1$ and k^* approximates 0.1.

We illustrate the first twenty orders of acfs and ccfs in [Figure 5](#) and [Figure 6](#) for the same parameter values used in the illustrations of the GAS²V-N model while considering two different values of the degrees of freedom, namely 11.8745 and 19.8387, which guarantee the same kurtoses of ϵ_t when $\epsilon_t \sim GED$ with $\nu = 1.5$ and $\nu = 1.7$, respectively. We observe that the autocorrelations and cross-correlations of the absolute values are smaller than those of GAS²V-N models for the considered parameter values. Moreover, larger degrees of freedom imply larger autocorrelations and larger cross-correlation of absolute values. Therefore, we may conclude that fatter tails of ϵ_t imply smaller autocorrelations of both absolute and squared returns, which coincides with the conclusion of [Carnero et al. \(2004\)](#).

2.2.3. GA V-GED

Finally, we assume that ϵ_t follows a $GED(\nu)$ distribution with probability density function (pdf) $f_{\nu}(\epsilon_t) = \frac{1}{2} \frac{\Gamma(\nu)}{\Gamma(\nu+1/2)} \exp(-\frac{1}{2} |\epsilon_t|^\nu)$ with $\nu = 2 - 2/\nu f(1/\nu)/f(3/\nu)$. Then u_t is given by (11) where $\eta_t = \frac{1}{2} |\epsilon_t|^\nu$ follows a Gamma $(2, 1/\nu)$ distribution; see [Harvey \(2013\)](#). The model defined by equations (1), (2), (7) and (11) are denoted as GAS²V-G. It is strictly stationary if $|k| < 1$ and if further $k + |k^*| < 1$, Y_t and $|Y_t|$ have finite and time-invariant moments of non-negative integer order c . Under these conditions, the acfs and ccfs are also finite. The analytical expressions of the two expectations are given in [Appendix A.3](#).

In Figure 2, we also plot the ratio of the kurtoses between GAS²V-G and ARSV(l) for the same parameter values specified for the GAS²V-N model while $\nu = 1.5$. Though this GAS²V-G always generates returns with higher kurtosis than the ARSV(l) model, its kurtosis is smaller than that of the corresponding GAS²V-N with similar parameter values. As the Gaussian distribution is a special case of the GED distribution with $\nu = 2$, we might conclude that a fatter tailed GED generates less kurtosis. Moreover, the ratio of GAS²V-G is indistinguishable from that of the GAS²V-T model when the return errors are assumed to have the same kurtosis in both models. Apparently, the kurtosis of the return generated by the GAS²V model depends on the kurtosis of the errors and barely on the type of distribution.

We also analyse the first order acfs and ccfs of the returns generated by the GAS²V-G model when $\nu = 1.5$ in Figure 3 and Figure 4. We find that when the kurtoses of return errors are the same as in GAS²V-T, these moments related with squared returns are indistinguishable for both models. The first order autocorrelation of absolute returns and first order cross-correlation between returns and future absolute returns of GAS²V-T models are larger than those of the GAS²V-G model.

Figure 5 and Figure 6 illustrate the first twenty orders of these moments for two different GAS²V-G models with two different values of the GED parameter, $\nu = 1.5$ and 1.7. As expected, the acfs of $|Y_t|$ and Y_t^2 have both an exponential decay. Furthermore, fatter tails of ε_t imply smaller autocorrelations, but it has very mild influence on the cross-correlations. It verifies again that the acf of squared returns and ccf between returns and future squared return are indistinguishable to those of GAS²V-T model with ε_t having the identical kurtosis.

3. MCMC estimation

3.1. Model estimation and comparison method

Due to the lack of observability of the volatilities, it is not possible to obtain an analytical expression of the likelihood function of SV models, which complicates the estimation of the parameters and underlying volatilities; see [Broto and Ruiz \(2004\)](#) for a survey on alternative procedures to estimate SV models. Fortunately, the user-friendly and freely available software BUGS provides a MCMC estimator which uses the Gibbs Sampling algorithm. There are two main versions of BUGS, namely WinBUGS and OpenBUGS. WinBUGS is an established and stable, stand-alone version, which is not further developed; see [Meyer and Yu \(2000\)](#) for a description of WinBUGS and [Yu \(2012\)](#) and [Wang et al. \(2013\)](#) for its application. In this paper, we adopt OpenBUGS that is still being developed and refer to [Mao et al. \(2013\)](#) for the detailed algorithms.

To compare two competitive models, saying M_0 and M_1 , we consider the Bayes Factor (BF). The BF, which is defined as the ratio of the marginal likelihood values of two competing models, $BF = \frac{p(y|M_1)}{p(y|M_0)}$, where $p(y|M_k)$ is the marginal likelihood of model k with $k = 0, 1$. If the prior odds ratio is 1 by Bayes' theorem, the posterior odds ratio takes the same value as the BF. [Jeffreys \(1961\)](#) gave a scale for the interpretation of BFs. If $\ln(BF)$ is less (bigger) than 0, there is evidence in favor of (against) M_0 . Moreover, if $\ln(BF) \in (0, 1)$, the evidence against M_0 is barely worth mention; if $\ln(BF) \in (1, 3)$, the evidence against M_0 is positive; if $\ln(BF) \in (3, \infty)$ (Or $(-\infty, -3)$), the evidence against M_0 is strong (or very strong).

3.2. Sampling performance

To check the reliability of this MCMC estimator, we simulate data from the three GAS²V models, GAS²V-N, GAS²V-T and GAS²V-G, with parameter values

$\{JL, e/\sigma, u, a, k^*, v, v_0\} = \{0, 0.98, 0.05, 0.07, 0.08, 1.5, 11.8745\}$ while imposing the restriction $k = 0$. Recall that, in the previous section, we show that the GAS²V-G and GAS²V-T model generate returns with very similar properties when the parameters of both distributions are chosen to have the same kurtoses. Hence, there could be potential identification problem. Therefore, we consider the restricted GAS²V models in the rest of the paper. For each model, $T = 1000$ observations are simulated. The posterior mean and standard deviation of each parameter in the model is obtained by fitting the model to these simulated data using the MCMC estimator. The total number of iterations is 30,000 with the first 10,000 iterations used as burn-in. We replicate the experiment for $r = 200$ times.

Table 1 reports the Monte Carlo average of these posterior means and standard deviations together with the standard deviation of these posterior means based on these r replicates for each model. We find that the MCMC estimator is quite reliable for all parameters in all cases.

4. Empirical application

4.1. Estimation results from daily data

In this subsection, we fit the restricted GAS²V models to one daily mean-adjusted return series, namely S&P500, observed from September 1, 1998 till July 25, 2014 with $T = 4000$ observations. The same data is analysed in Mao et al. (2013) and fitted to models of the GASV family.

Table 2 reports the posterior mean, the 95% credible interval for each parameter and the marginal log-likelihood. From the table, several conclusions can be drawn. First, all the parameter estimates are different from zero. The credible intervals of the degrees of freedom in both GAS²V-T and GAS²V-G model exclude the case of the Normal distribution, which implies that the return error follows a fat-tailed

distribution. Regarding the goodness of fit of the models, we observe, analysing the log-likelihood values, that GAS²V-N model is outperformed by the other two models and that the GAS²V-T model fits the data better than the GAS²V-G model. However, the preference is negligible.

4.2. Estimation results from weekly data

In this subsection, we fit the restricted GAS²V models to the series of mean-adjusted S&P500 and NIKKEI225 weekly returns observed from January 13, 1992 to December 27, 2010. The number of observations are $T_1 = 990$ and $T_2 = 986$, respectively. Although the sample size is relatively small, according to our Monte Carlo experiments, we can obtain reliable estimation results. For completeness, we also fit two GASV models, namely, T-GASV-G and T-GASV-N, to these two series. Some relevant sample statistics are reported in [Table 3](#). We observe that the sample autocorrelations of the squared returns are significantly positive and the cross-correlations between returns and future squared returns are significantly negative, confirming the volatility clustering and leverage effect.

Estimation results are reported in [Table 4](#). According to the log-likelihood, the GAS²V-G model fits the S&P500 returns the best while T-GASV-G provides the best fit to both S&P500 and NIKKEI225 series of returns. However, the advantage of this model compared to the others is barely worth mention.

4.3. Forecasting results from weekly data

A model good in-sample performance does not necessarily imply a model good out-of-sample performance. In this section, we compare the out-of-sample performance of the proposed models using the two weekly return series described above. The three GAS²V models and two GASV models are fitted to the return data and used to obtain one-period-ahead out-of-the-sample forecasts of weekly volatility. We split the weekly

sample into an in-sample estimation period and an out-of-sample forecast evaluation period. For estimation we use the rolling window scheme, where the size of the sample, which is used to estimate the competing models, is fixed at T_i with $i = 1$ and 2 . The first forecast is made for the first week of January, 2011. When a new observation is added to the sample, we discard the first observation and re-estimate all the models. The re-estimated models are then used to forecast volatility. This process is repeated until we reach the end of the sample, December 30, 2013. In total, we obtain 157 forecasts from each model.

Two alternative criteria are considered in this paper to compare the out-of-sample performances of these models, namely Mean Absolute Error (MAE) of the volatility forecasts and the Log Predictive Score (LPS), which is computed using the MCMC output. In Table 5, we report the MAE of the volatility forecasts. First, we calculated the weekly realized volatility (RV) obtained from the sum of daily squared returns. Let RV_t denote the weekly RV and $p(t, k)$ denote the k -th daily log-price in week t . Then RV_t is defined as $\frac{1}{N_t} \sum_{k=1}^{N_t} (p(t, k) - p(t, k-1))^2$, where N_t is the number of trading days in week t and $p(t, 0) = p(t-1, N_{t-1})$. We match each volatility forecast with the corresponding realized volatility. Table 5 summarizes the MAE of the volatility forecasts. We can see that all the models perform nearly equally in forecasting the volatility of the S&P500 and NIKKEI225 returns.

On the other hand, LPS is a scoring rule introduced by Good (1952) that examines the model's performance when its implied predictive distribution is compared with observations not used in the inference sample. In this sense, it evaluates the out-of-sample behaviour of different models by mean of their divergence between the actual sampling density and the predictive density. The formula for the LPS is given as follows

$$LPS = K \frac{1}{T} \sum_{k=1}^T \log(f(Y_{T+k|Y_k}, \dots, Y_{T+k-1})), \quad (13)$$

where K is the total number of forecasts we've obtained. The one-step-ahead LPS are reported in the lower panel of [Table 5](#). Again, it seems that these different models provide very similar forecasts.

5. Conclusion

In this paper, we propose a new score driven stochastic volatility model, named GAS²V, in the spirit of the proposal of [Creal et al. \(2013\)](#) and [Harvey \(2013\)](#). Particularly, three different GAS²V are considered, depending on the return error distribution, named GAS²V-N if the error distribution is Normal, GAS²V-T if it is Student-t and GAS²V-G if the return error follows a GED distribution. The closed-form expressions of the marginal variance, kurtosis, autocorrelations of power-transformed absolute returns and cross-correlations between returns and future power-transformed absolute returns are obtained for these models. The GAS²V models are included in the GASV family and therefore are flexible to represent the empirical features of the data. Moreover, the GAS²V-T and GAS²V-G can represent very similar properties when the kurtosis of the return error is fixed. Therefore, there can be problem of identification of the parameters. Through Monte Carlo studies, we show that the MCMC estimator implemented by BUGS is able to estimate the parameters of some restricted GAS²V models adequately. These restricted GAS²V models are fitted to both daily and weekly financial data and we observe that the GAS²V-T model provides the best fit in-sample for the daily S&P500 return series. Regarding the out-of-sample performance of the models in forecasting the volatility of the weekly financial returns of the S&P500 and NIKKEI225, all models provide similar mean absolute forecast errors when the volatility forecasts are compared with a consistent measure of volatility, the realized volatility. The same conclusion is obtained when we consider the alternative Log Predictive Score criterion. We leave for future research

the comparison of the GAS^2V models with the robust GARCH models such as the Beta-t-EGARCH and Gamma-GED-GASV models of [Harvey \(2013\)](#). Moreover, the analysis of the robustness of our GAS^2V models in front of outliers is in our research agenda.

Figures and Tables

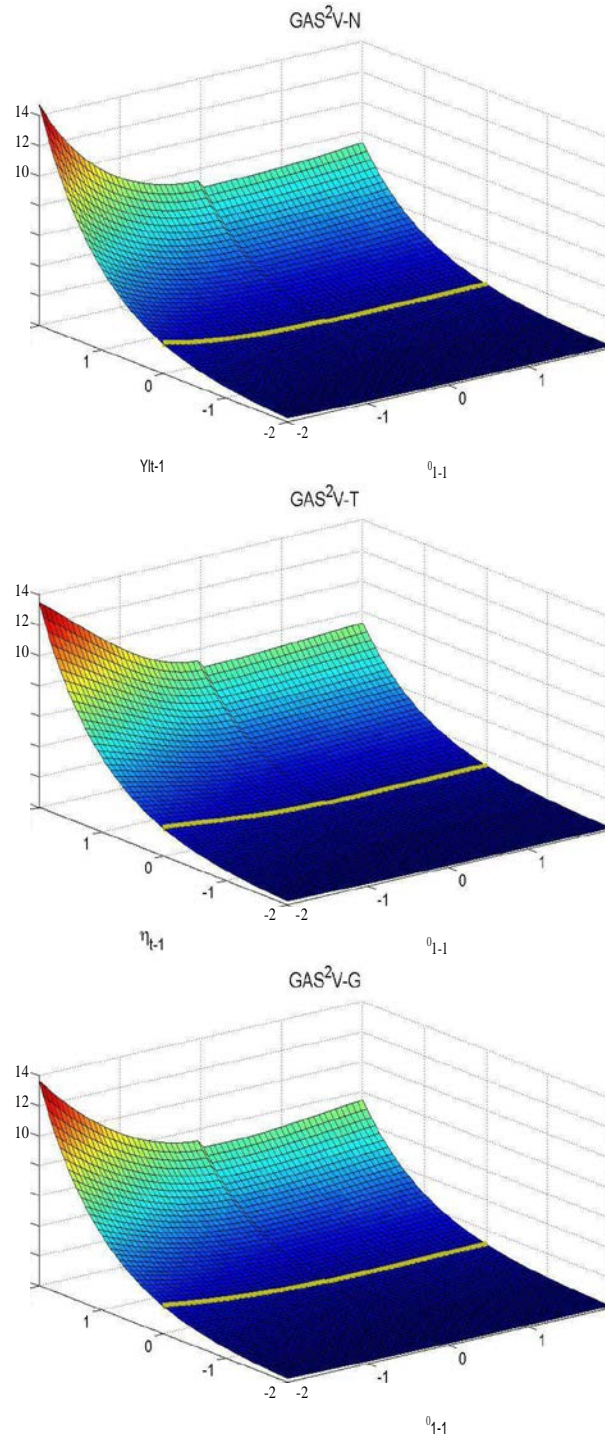


Figure 1: SNIS of $\text{GAS}^2\text{V-N}$ (top panel) with parameters $(a, cf, k^*, k, u) = (0.07, 0.98, 0.08, 0.1, 0.05)$ and $\exp((1 - cf)J/L)u; < > = 1$, $\text{GAS}^2\text{V-T}$ (middle panel) with $V_0 = 6$ and $\text{GAS}^2\text{V-G}$ (bottom panel) with $\nu = 1.5$

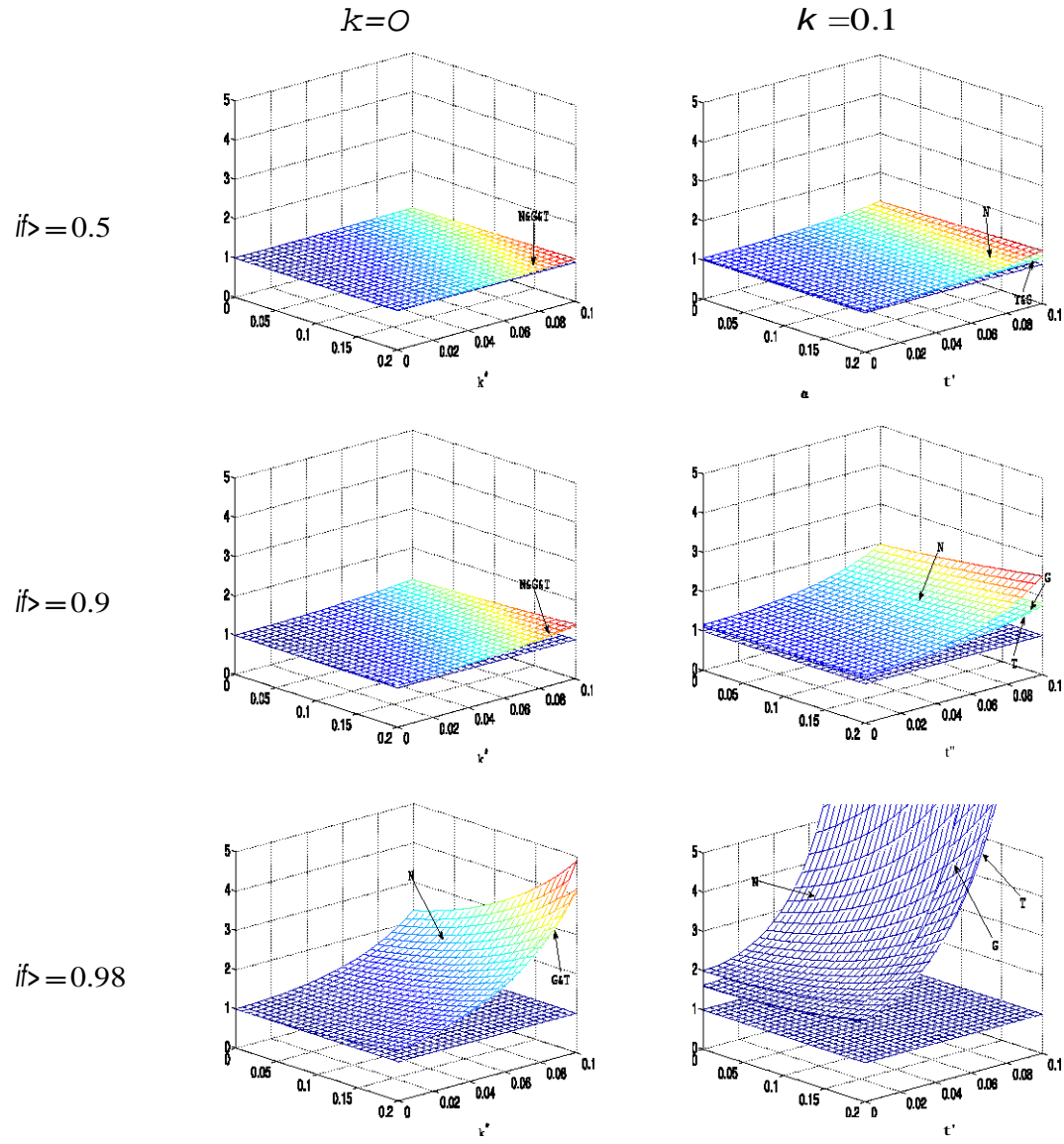


Figure 2: Ratio between the kurtoses of the GAS²V model and the symmetric ARSV(1) model with Gaussian (N), GED (G) and Student-t (T) errors when $k = 0$ (left column) and 0.1 (right column) for three different values of the persistence parameter, $if \geq 0.5$ (first row), $if \geq 0.9$ (middle row) and $if \geq 0.98$ (bottom row).

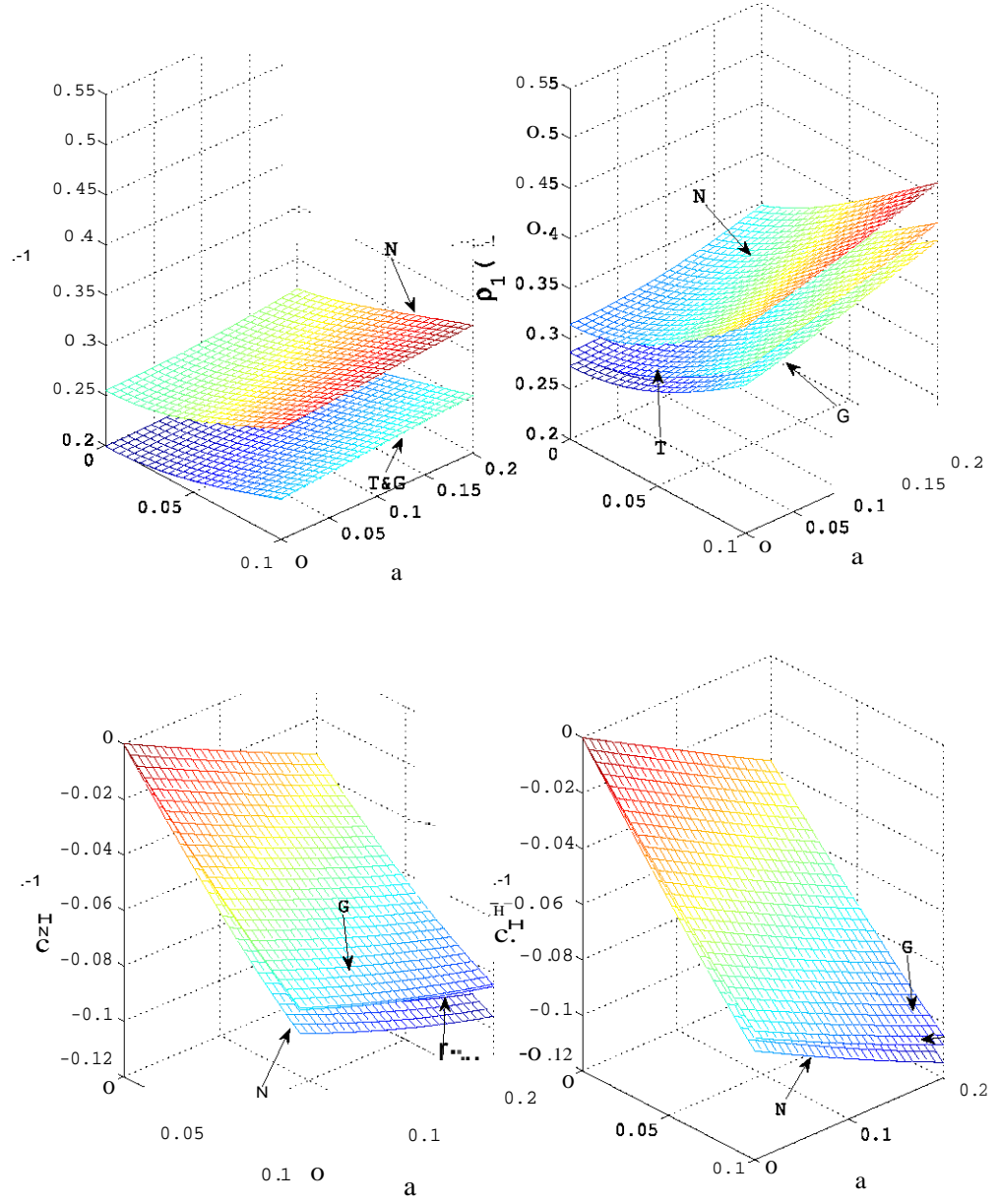


Figure 3: First order autocorrelations of squares (top left), first order autocorrelations of absolute returns (top right), first order cross-correlations between returns and future squared returns (bottom left) and first order cross-correlations between returns and future absolute returns (bottom right) of different GAS²V models when $h = 0$, $r^p = 0.98$, $a = 0.05$, $v = 1.5$, $v_0 = 11.8745$ and $k = 0$. The surface N represents the moments of the GAS²V-N model, T represents the moments of the GAS²V-T model and G represents the moments of the GAS²V-G model.

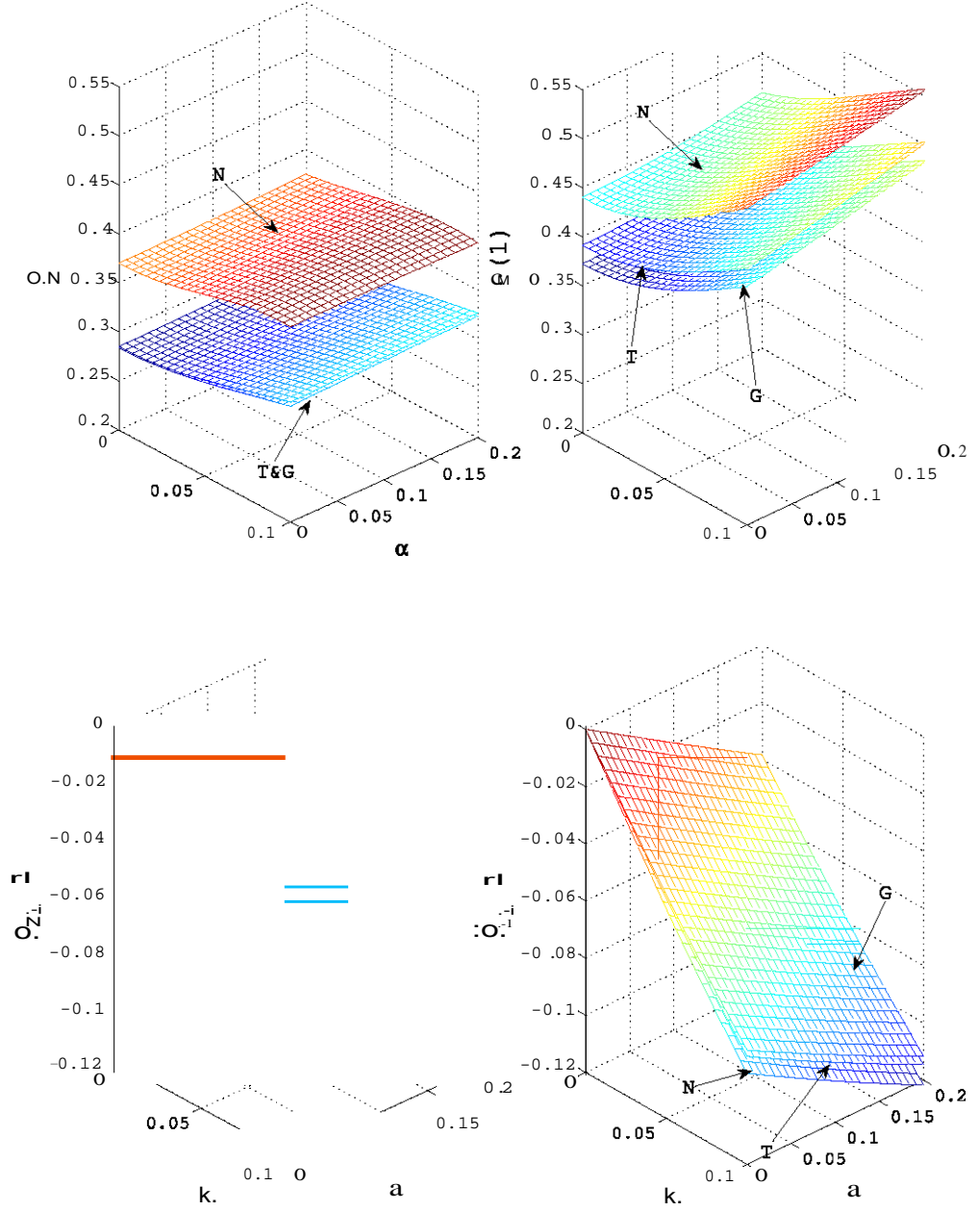


Figure 4: First order autocorrelations of squares (top left), first order autocorrelations of absolute returns (top right), first order cross-correlations between returns and future squared returns (bottom left) and first order cross-correlations between returns and future absolute returns (bottom right) of different GAS²V models when $J_i = 0$, $r_j = 0.98$, $\alpha = 0.05$, $\nu = 1.5$, $V_0 = 11.8745$ and $k = 0.1$. The surface N represents the moments of the GAS²V-N model, T represents the moments of the GAS²V-T model and G represents the moments of the GAS²V-G model.

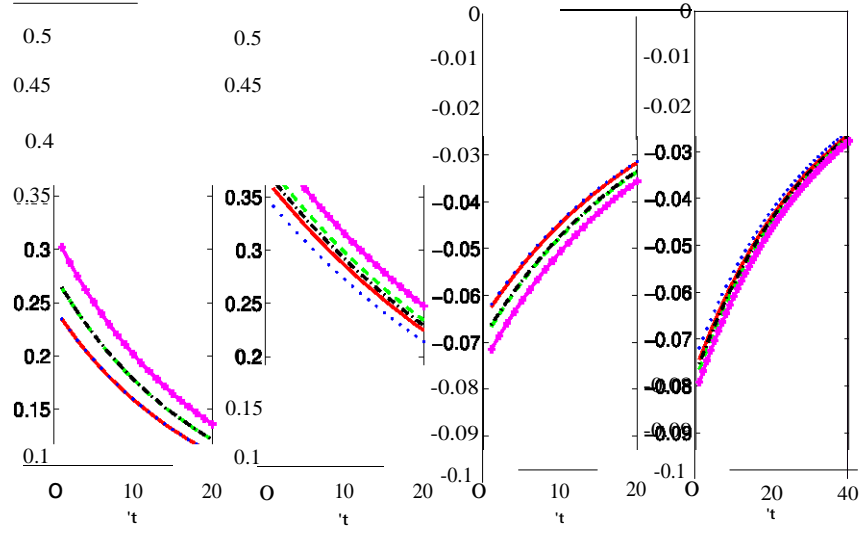


Figure 5: Autocorrelations of squares (first column), autocorrelations of absolute returns (second column), cross-correlations between returns and future squared returns (third column) and cross-correlations between returns and future absolute returns (fourth column) for different specifications of GAS²V models when $4J = 0.98$, $\mu = 0.05$, $\alpha = 0.07$, $k^* = 0.08$ and $k = 0$. The solid line corresponds to the moments of the GAS²V-T model with $\nu_0 = 11.8745$ while $\nu_0 = 19.8387$ for dashed lines. The dotted and dashdot lines corresponds to the moments of the GAS²V-G model when $\nu = 1.5$ and 1.7 , respectively. Finally, the '+-' line represents the moments of the GAS²V-N model.

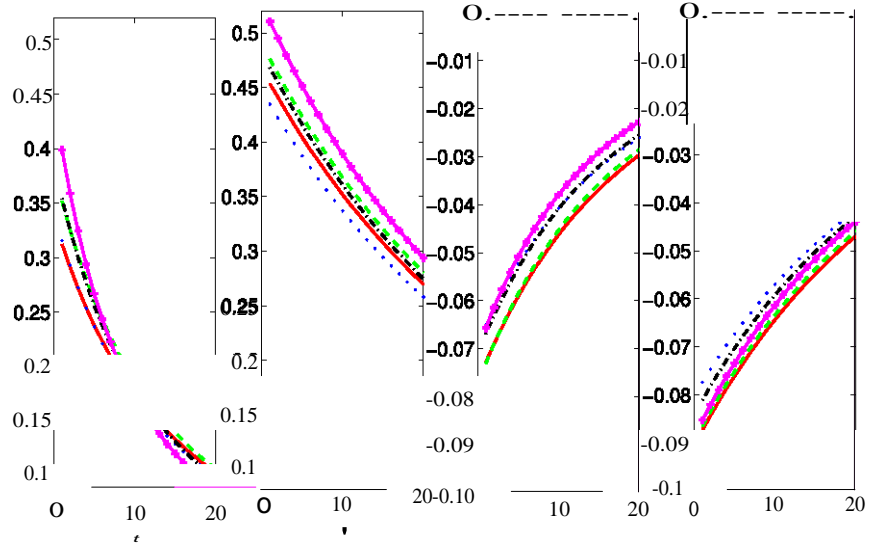


Figure 6: Autocorrelations of squares (first column), autocorrelations of absolute returns (second column), cross-correlations between returns and future squared returns (third column) and cross-correlations between returns and future absolute returns (fourth column) for different specifications of GAS²V models when $rjJ = 0.98$, $\alpha = 0.05$, $a = 0.07$, $k^* = 0.08$ and $k = 0.1$. The solid line corresponds to the moments of the GAS²V-T model with $\nu_0 = 11.8745$ while $\nu_0 = 19.8387$ for dashed lines. The dotted and dashdot lines corresponds to the moments of the GAS²V-G model when $\nu = 1.5$ and 1.7 , respectively. Finally, the '+' line represents the moments of the GAS²V-N model.

	μ'	ϕ	α	k^*	σ^2	ν
GAS²V-N						
True	0	0.98	0.07	0.08	0.06	
Mean	0.131 (1.259)	0.976 (0.010)	0.067 (0.056)	0.083 (0.021)	0.054 (0.018)	
s.d.	1.548	0.007	0.060	0.020	0.014	
GAS²V-T						
True	0	0.98	0.07	0.08	0.05	11.8745
Mean	0.108 (1.274)	0.974 (0.010)	0.076 (0.056)	0.084 (0.026)	0.059 (0.027)	10.602 (2.007)
s.d.	1.362	0.008	0.058	0.022	0.016	2.845
GAS²V-G						
True	0	0.98	0.07	0.08	0.05	1.5
Mean	0.257 (1.438)	0.973 (0.011)	0.071 (0.073)	0.081 (0.029)	0.055 (0.025)	1.522 (0.147)
s.d.	1.529	0.008	0.067	0.024	0.016	0.104

Table 1: Monte Carlo results of the MCMC estimator of the parameters of the GAS²V model. The value reported are the Monte Carlo average and standard deviation (in parenthesis) of the posterior means together with the Monte Carlo average of the posterior standard deviation.

	GAS ² V-N	GAS ² V-T	GAS ² V-G
μ	-2.401 (-3.530, -0.215)	-1.435 (-1.782, -0.669)	-1.892 (-2.518, -0.169)
σ	0.978 (0.966, 0.989)	0.980 (0.968, 0.989)	0.982 (0.973, 0.992)
γ	0.104 (0.003, 0.145)	0.080 (0.048, 0.108)	0.067 (0.050, 0.093)
κ	0.056 (0.041, 0.071)	0.087 (0.069, 0.104)	0.073 (0.060, 0.080)
ω	0.020 (0.009, 0.030)	0.011 (0.007, 0.021)	0.008 (0.001, 0.002)
ν		3.929 (2.733, 3.176)	1.395 (1.267, 1.422)
Log-Likelihood	-6.070	-5.853	-5.900

Table 2: Estimation results from daily S&P500. The values reported are the mean and 95% credible interval (parenthesis) of the posterior distributions.

	Median	Maximum	Minimum	Std. Dev.	Skewness	Kurtosis	P2(1)	P1(1)	P21(1)	Pn(1)
S&P500	0.125	11.245	-20.195	2.404	-0.813 ^{***}	10.354...	0.297*	0.332*	-0.254*	-0.229*
NIKKEI225	0.136	11.529	-27.805	3.113	-0.741*	9.945 ^{***}	0.120 ^{***}	0.171 ^{***}	-0.125 ^{***}	-0.139 ^{***}

^{***} Significant at 1% level.

Table 3: Sample moments of mean adjusted weekly S&P500 and NIKKEI225 returns observed from Jan 13, 1992 to Dec 27, 2010.

11
00
11

Data	Model	Log MargLik	μ	σ	α	β	γ	δ
S&P500	GAS ² V-N	-1.579	-2.534	0.964	0.030	(0.013, 0.047)	(0.204, 0.380)	(-0.015, 0.037)
				(-3.914, -1.171)	(0.947, 0.982)	0.205	0.022	15.490
	GAS ² V-T	-1.629	-2.032	0.971	0.018	{0.1375, 0.3335}	(-0.005294, 0.04658)	(9.894, 20.05)
			(-3.651, -1.097)	{0.9542, 0.9839}	(0.004856, 0.02706)	0.245	0.014	2.010
	GAS ² V-G	-1.577	-2.419	0.966	0.029	(0.106, 0.339)	(-0.017, 0.051)	{1.802, 2.215}
			(-5.262, -0.492)	(0.937, 0.982)	(0.015, 0.054)	0.230	-0.047	
NIKKEI225	T-GASV-N	-1.579	-1.548	0.962	0.032	(0.09363, 0.3669)	(-0.1132, 0.007123)	
			(-3.576, 0.09023)	(0.9436, 0.974)	(0.01539, 0.05349)	0.221	-0.058	2.257
	T-GASV-G	-1.527	-1.394	0.957	0.040	{0.07043, 0.353}	(-0.1335, 0.02006)	{1.969, 2.526}
			(-4.066, 0.516)	{0.9283, 0.9788}	{0.01514, 0.07397}	0.164	0.057	
	GAS ² V-N	-7.975	1.288	0.882	0.060	(0.024, 0.306)	(0.006, 0.107)	
			(0.599, 1.873)	(0.832, 0.932)	(0.029, 0.105)	0.090	0.074	13.050
	GAS ² V-T	-7.559	1.505	0.917	0.033	(-0.024, 0.222)	(0.029, 0.112)	(8.252, 21.04)
			(0.821, 2.125)	(0.848, 0.957)	(0.015, 0.065)	0.152	0.064	2.002
	GAS ² V-G	-7.966	1.348	0.877	0.064	(0.016, 0.276)	(0.025, 0.114)	(1.824, 2.252)
			(0.793, 2.017)	(0.797, 0.929)	(0.031, 0.119)	0.041	-0.150	
	T-GASV-N	-7.523	1.800	0.893	0.059	(-0.175, 0.258)	(-0.276, -0.041)	
			(0.700, 2.630)	(0.833, 0.932)	(0.033, 0.100)	0.030	-0.158	2.164
	T-GASV-G	-7.208	1.897	0.873	0.074	(-0.170, 0.229)	(-0.273, -0.055)	(1.964, 2.518)
			(1.068, 2.666)	(0.801, 0.924)	(0.039, 0.126)			

Table 4: MOMO estimates of parameters of GAS²V and GASV models fitted to weekly S&P500 and NIKKEI225. The values reported are the mean and, in parentheses, 95% credible intervals of the posterior distributions.

MAE*1000					
	GAS ² V-N	GAS ² V-T	GAS ² V-G	T-GASV-N	T-GASV-G
S&P500	6.220	6.378	6.248	6.206	6.220
NIKKEI 225	9.171	9.536	9.157	9.235	8.992
LPS					
S&P500	-2.047	-2.047	-2.064	-2.049	-2.062
NIKKEI 225	-2.572	-2.524	-2.764	-2.579	-2.672

Table 5: Forecasting results from weekly data. MAE refers to the mean absolute forecasting error and LPS refers to the log-predictive likelihood.

Appendix A. Closed-form of $E(\exp(bf(e)))$ and $E(\text{letlcexp}(bf(e)))$

Appendix A.1. Et Normal

Proposition 1. Let e be a non-negative integer and $b \in \mathbb{R}$ and E_t and $f(E_t)$ are defined as in GAS²V-N model. If $bk + \text{lbk} \leq 1$, then

$$E(\text{letlc} \exp(bj(E_t))) = \frac{\exp(-bk)}{2} \left(\frac{e+1}{2} \right)^{\frac{1}{2}} \left[\exp(ba) \left(\frac{1}{2} \right)^{-b(k+k^*)} + \left(\frac{1}{2} \right)^{-b(k-k^*)} \right] \quad (\text{A.1})$$

and

$$E(E \exp(bj(E_t))) = \exp(-k) \left(\frac{e+1}{2} \right)^{\frac{1}{2}} \left[\exp(ba) \left(\frac{1}{2} \right)^{-b(k+k^*)} + \left(\frac{1}{2} \right)^{-b(k-k^*)} \right] \quad (\text{A.2})$$

Proof.

$$= \frac{1}{2} \left(\int_{-\infty}^{\infty} \exp(ba + bke - bk + bk^*E) \exp(-sE) dE \right)$$

$$E(\text{letlc} \exp(bf(E_t)))$$

$$+ \int_{-\infty}^{\infty} \exp(b(a-k)) \exp(bkE - bk - bk^*E) \exp(-sE) dE, \quad (\text{A.3})$$

Integrating by substitution with $s = -E$, in the finite integral, we obtain

$$E(\text{letlc} \exp(bf(E_t))) = \frac{1}{2} \exp(b(a-k)) \int_{-\infty}^{\infty} \exp(-bk) \exp(-bk^*E) \exp(-sE) dE$$

$$= \int_0^{\infty} \int_{\mathbb{R}^d} \log(s) \exp((b(k+k^*)-2)s) ds + \int_0^{\infty} \int_{\mathbb{R}^d} \log(Et) \exp((b(k-k^*)-2)E) dE, .$$

(A.4)

According to the formula 3.326-2 of [Ryzhik et al. \(2007\)](#), when $c \geq 0$ and $b(k + |k^*|) < 1$ the former equation reduces to

$$E(\epsilon_t^c \exp(bf(\epsilon_t))) = \frac{\exp(b(\alpha - k))}{\sqrt{2\pi}} \frac{\Gamma(\frac{c+1}{2})}{2(1 - b(k + k^*))^{\frac{c+1}{2}}} + \frac{\exp(-bk)}{\sqrt{2\pi}} \frac{\Gamma(\frac{c+1}{2})}{2(1 - b(k - k^*))^{\frac{c+1}{2}}} \\ = \frac{\exp(b(\alpha - k))}{\sqrt{2\pi}} \frac{\Gamma(\frac{c+1}{2})}{2(1 - b(k + k^*))^{\frac{c+1}{2}}} + \frac{\exp(-bk)}{\sqrt{2\pi}} \frac{\Gamma(\frac{c+1}{2})}{2(1 - b(k - k^*))^{\frac{c+1}{2}}} \quad (A.5)$$

Following the same steps, we can obtain the analytical expression of $E(\epsilon_t^c \exp(bj(\epsilon_t)))$ as follows:

$$E(\epsilon_t^c \exp(bf(\epsilon_t))) \\ = \int_{-\infty}^0 \epsilon_t^c \exp(b\alpha + bk\epsilon_t^2 - bk + bk^*\epsilon_t^2) \frac{1}{\sqrt{2\pi}} \exp\left(-\frac{\epsilon_t^2}{2}\right) d\epsilon_t \\ + \int_0^{\infty} (\epsilon_t)^c \exp(bk\epsilon_t^2 - bk - bk^*\epsilon_t^2) \frac{1}{\sqrt{2\pi}} \exp\left(-\frac{\epsilon_t^2}{2}\right) d\epsilon_t \\ = \frac{\exp(b(\alpha - k))}{\sqrt{2\pi}} \int_0^{\infty} (-s_t)^c \exp((b(k + k^*) - \frac{1}{2})s_t^2) ds_t \\ + \frac{\exp(-bk)}{\sqrt{2\pi}} \int_0^{\infty} (\epsilon_t)^c \exp((b(k - k^*) - \frac{1}{2})\epsilon_t^2) d\epsilon_t \\ = \frac{\exp(b(\alpha - k))}{\sqrt{2\pi}} \frac{(-1)^c \Gamma(\frac{c+1}{2})}{2(1 - b(k + k^*))^{\frac{c+1}{2}}} + \frac{\exp(-bk)}{\sqrt{2\pi}} \frac{\Gamma(\frac{c+1}{2})}{2(1 - b(k - k^*))^{\frac{c+1}{2}}} \\ = \frac{\exp(-bk)}{2\sqrt{2\pi}} \Gamma\left(\frac{c+1}{2}\right) \left[(-1)^c \exp(b\alpha) \left(\frac{1}{2} - b(k + k^*)\right)^{-\frac{c+1}{2}} + \left(\frac{1}{2} - b(k - k^*)\right)^{-\frac{c+1}{2}} \right]. \quad (A.6)$$

D

Appendix A.2. $t \rightarrow \infty$

Proposition 2. Let e be a nonnegative integer and $b \in \mathbb{R}$ and $\lambda > 0$ and $J(t)$ defined as in GASJ V-T model, then when $\nu > e$

$$E(e^{\lambda t} \exp(-b f_t)) = \frac{(\nu - 2)^e \exp(-b k) B(\frac{1}{2}, \frac{\nu}{2})}{2^{e+1} \Gamma(\frac{\nu}{2})} \cdot \left\{ \sum_{p=0}^e \frac{(-1)^p}{p!} \left[1 + E \left(\prod_{i=1}^p (e + 1 + 2j_i) \frac{(b(\nu + 1)(k + k^*))^{j_i}}{j_i!} \right) \right] \right. \\ \left. + \left[1 + E \left(\prod_{i=1}^e (e + 1 + 2j_i) \frac{(b(\nu + 1)(k - k^*))^{j_i}}{j_i!} \right) \right] \right\} \quad (A.7)$$

and

$$E(e^{\lambda t} \exp(-b f_t)) = \frac{(\nu - 2)^e \exp(-b k) B(\frac{1}{2}, \frac{\nu}{2})}{2^{e+1} \Gamma(\frac{\nu}{2})} \cdot \left\{ (-1)^e \exp(ba) \left[1 + E \left(\prod_{i=1}^e (e + 1 + 2j_i) \frac{(b(\nu + 1)(k + k^*))^{j_i}}{j_i!} \right) \right] \right. \\ \left. + \left[1 + E \left(\prod_{i=1}^e (e + 1 + 2j_i) \frac{(b(\nu + 1)(k - k^*))^{j_i}}{j_i!} \right) \right] \right\}. \quad (A.8)$$

Proof. The probability density function of f_t is $f(f_t; t) = \frac{J(f_t; t)}{J_0(t; t)} (1 + \frac{f_t}{2})^{-\frac{\nu}{2}}$ where $J_0(t; t) = \frac{2^{\frac{\nu}{2}} \Gamma(\frac{\nu}{2})}{\sqrt{\pi}}$, then $\lambda f_t = (\nu + 1)b f_t - 1$ and $\lambda f_t = \frac{E(f_t)}{J_0(f_t; t)} \dots B e t a(\frac{1}{2}, \frac{\nu}{2})$, see [Harvey \(2013\)](#).

$$\begin{aligned}
E(I E t l e \exp(b j(E,))) &= \int_0^\infty \left(-E, \right) e \exp(b(a-k)) \exp(b(v+1)(k+k^*)b,) 1/ >_0(E,) dE, \\
&+ \int_0^\infty E \exp(-bk) \exp(b(v+1)(k-k^*)b,) 1/ >_0(Et) dEt \\
&= \exp(b(a-k)) \int_0^\infty E \exp(b(v+1)(k+k^*)b,) 1/ >_0(Et) dEt \\
&+ \exp(-bk) \int_0^\infty E \exp(b(v+1)(k-k^*)b,) 1/ >_0(Et) dEt \\
&= \exp(b(a-k)) \int_0^\infty E (I E t l e \exp(b(v+1)(k+k^*)b,)) \\
&\quad + \exp(-bk) E (I E t l e \exp(b(v+1)(k-k^*)b,)), \quad (A.9)
\end{aligned}$$

We proceed to work out the expectation $E(\text{IEtle exp}(\text{mb},))$ with respect to E_{\cdot} . Note that $E(\text{IEtle exp}(\text{mb},)) = \text{cp}0 E(\text{vef}^2 b^2 / (1-b,)^2 \exp(\text{mb},))$ with respect to b , $\text{BetaG}(\cdot)$. It follows that

[illegible]

with the expectation taken with respect to a $Beta(e, v - e)$ when $v > e$, which is the moment generating function of b , $Beta(e, v - e)$. It yields that

$$E(I E t l e \exp (m b,)) = P o v e / 2 \quad B e t a (2, \bar{2}) \quad \{ \quad \quad \quad \} \quad (A.11)$$

Combining equation (A.9) and (A.11) gives the expression. On the other hand,

$$\begin{aligned}
E(E \exp(bj(Et))) &= \int_0^\infty E \exp(b(a-k)) \exp(b(v+1)(k+k^*)bt) \frac{1}{\Gamma(v)} dt \\
&+ \int_0^\infty E \exp(-bk) \exp(b(v+1)(k-k^*)bt) \frac{1}{\Gamma(v)} dt \\
&= (-1)^v \exp(b(a-k)) \int_0^\infty E \exp(b(v+1)(k+k^*)bt) \frac{1}{\Gamma(v)} dt \\
&+ \exp(-bk) \int_0^\infty E \exp(b(v+1)(k-k^*)bt) \frac{1}{\Gamma(v)} dt \\
&= (-1)^v \exp(b(a-k)) E \left(\frac{1}{2} \exp(b(v+1)(k+k^*)bt) \right) \\
&+ \frac{\exp(-bk)}{2} E \left(\frac{1}{2} \exp(b(v+1)(k-k^*)bt) \right) \quad (A.12)
\end{aligned}$$

The proof is completed. D

Appendix A.9. $f^{(v)}(GED(v))$

Proposition 3. Let v be a nonnegative integer and $b \in \mathbb{R}$. f_t and $f^*(t)$ defined as in GASJV-G model. Then, when $b(k+k^*) < 1/v$,

$$\begin{aligned}
E(f_t \exp(bf(Et))) &= \exp(b(a-k)) \frac{(r(1/v)t/2 - 1)^{v-1}}{(r(1/v)t/2)^{v-1}} (1 - vb(k+k^*))^{-1} \\
&+ \exp(-bk) \frac{(r(1/v)t/2 - 1)^{v-1}}{(r(1/v)t/2)^{v-1}} (1 - vb(k-k^*))^{-1} \quad (A.13)
\end{aligned}$$

and

$$\begin{aligned}
E(f_t \exp(bj(Et))) &= (-1)^v \exp(b(a-k)) \frac{(r(1/v)t/2 - 1)^{v-1}}{(r(1/v)t/2)^{v-1}} (1 - vb(k+k^*))^{-1} \\
&+ \exp(-bk) \frac{(r(1/v)t/2 - 1)^{v-1}}{(r(1/v)t/2)^{v-1}} (1 - vb(k-k^*))^{-1} \quad (A.14)
\end{aligned}$$

Proof.

$$\begin{aligned}
& E(|\epsilon_t|^c \exp(bj(Et))) \\
&= \int_{-\infty}^{\infty} \left(\int_0^{\infty} \exp(ba + bkUt + bk^*(ut + 1))' l(l(Et)) dEt + 1 + \int_0^{\infty} \exp(bkut - bk^*(ut + 1))' l(l(Et)) dEt \right) \\
&= \exp(b(a - k)) \int_0^{\infty} E \exp(b(k + k^*)'igt)' l(J(Et)) dEt + \exp(-bk) \int_0^{\infty} E \exp(b(k - k^*)'igt)' l(J(Et)) dEt \\
&= \exp(b(a - k)) E(|\epsilon_t|^c \exp(b(k + k^*)'gt)) + \exp(-bk) E(|\epsilon_t|^c \exp(b(k - k^*)'gt)) \\
&= \frac{E(cpcg[\exp(b(k + k^*)'igt)])}{2} + \frac{E(cpcg[\exp(b(k - k^*)'igt)])}{2} \\
&= \frac{2}{9t} \exp \left(\frac{2}{9t} + \frac{2}{2} \right) \exp \left(\frac{2}{9t} \right)
\end{aligned}$$

According to the Appendix B.2 of [Harvey \(2013\)](#), when $E(\exp(b(k + k^*)Hgt)) < \infty$ and $E(\exp(b(k - k^*)gt)) < \infty$, the previous equation can be written

$$\frac{cpcexp(b(a - k))}{2} \frac{\Gamma(\frac{c}{2})}{\Gamma(\frac{c}{2})} \exp \left(\frac{\nu b(k + k^*)}{2} \right) + \frac{cpcexp(-bk)}{2} \frac{\Gamma(\frac{c}{2})}{\Gamma(\frac{c}{2})} \exp \left(\frac{\nu b(k - k^*)}{2} \right)$$

where $Y_t \sim \text{Gamma}(2, c^{-1})$. When $b(k + k^*) < 1$ both $E(\exp(b(k + k^*)Hgt))$ and $E(\exp(b(k - k^*)gt))$ are finite and given by the generating moments function of the Gamma distribution, then

$$\begin{aligned}
E(|\epsilon_t|^c \exp(bf(\epsilon_t))) &= \frac{\exp(b(a - k))}{2} \frac{(\Gamma(1/\nu))^{c/2-1} \Gamma(\frac{c+1}{\nu})}{(\Gamma(\frac{3}{\nu}))^{c/2}} (1 - \nu b(k + k^*))^{-\frac{c+1}{\nu}} \\
&+ \frac{\exp(-bk)}{2} \frac{(\Gamma(1/\nu))^{c/2-1} \Gamma(\frac{c+1}{\nu})}{(\Gamma(\frac{3}{\nu}))^{c/2}} (1 - \nu b(k - k^*))^{-\frac{c+1}{\nu}}
\end{aligned}$$

The expression for $E(|\epsilon_t|^c \exp(bj(Et)))$ can be obtained following the similar steps. D

References

Abanto-Valle, C., Bandyopadhyay, D., Lachos, V., Enriquez, I., 2010. Robust Bayesian analysis of heavy-tailed stochastic volatility models using scale mixtures

- of normal distributions. *Computational Statistics & Data Analysis* 54, 2883-2898.
- Asai, M., McAleer, M., 2011. Alternative asymmetric stochastic volatility models. *Econometric Reviews* 30, 548-564.
- Bollerslev, T., 1986. Generalized autoregressive conditional heteroskedasticity. *Journal of econometrics* 31, 307-327.
- Bollerslev, T., 1987. A conditionally heteroskedastic time series model for speculative prices and rates of return. *The Review of Economics and Statistics* , 542-547.
- Broto, C., Ruiz, E., 2004. Estimation methods for stochastic volatility models: A survey. *Journal of Economic Surveys* 18, 613-649.
- Cappuccio, N., Lubian, D., Raggi, D., 2004. MCMC Bayesian estimation of a skew-GED stochastic volatility model. *Studies in Nonlinear Dynamics & Econometrics* 8.
- Carnero, M., Peña, D., Ruiz, E., 2004. Persistence and kurtosis in GARCH and stochastic volatility models. *Journal of Financial Econometrics* 2, 319-342.
- Cavaliere, G., 2006. Stochastic volatility: Selected readings. *The Economic Journal* 116, F326-F327.
- Chen, C., Liu, F., So, M., 2008. Heavy-tailed-distributed threshold stochastic volatility models in financial time series. *Australian & New Zealand Journal of Statistics* 50, 29-51.
- Choy, B., Wai, Y., Chan, C., 2008. Bayesian Student-t stochastic volatility models via scale mixtures. *Advances in Econometrics* 23, 595--618.
- Crea!, D., Koopman, S.J., Lucas, A., 2013. Generalized autoregressive score models with applications. *Journal of Applied Econometrics* 28, 777-795.

- Durbin, J., Koopman, S.J., 1997. Monte cario maximum likelihood estimation for non-gaussian state space models. *Biometrika* 84, 669-684.
- Engle, R., Ng, V., 1993. Measuring and testing the impact of news on volatility. *The Journal of Finance* 48, 1779-1801.
- Engle, R.F., 1995. *ARCH: selected readings*. Oxford University Press.
- Ghysels, E., Harvey, A., Renault, E., 1996. Stochastic Volatility, in: Maddala, G.S., Rao, C.R., Vinod, H.D. (Eds.), *Statistical Methods in Finance*. Amsterdam: North-Holland.
- Giraitis, L., Leipus, R., Surgailis, D., 2007. Recent advances in arch modelling, in: *Long memory in economics*. Springer, pp. 3-38.
- Good, I.J., 1952. Rational decisions. *Journal of the Royal Statistical Society. Series B (Methodological)* , 107-114.
- Harvey, A., 2013. *Dynamic Models for Volatility and Heavy Tails: With Applications to Financial and Economic Time Series*. Cambridge University Press.
- Harvey, A., Ruiz, E., Shephard, N., 1994. Multivariate stochastic variance models. *The Review of Economic Studies* 61, 247-264.
- Harvey, A., Shephard, N., 1996. Estimation of an asymmetric stochastic volatility model for asset returns. *Journal of Business & Economic Statistics* 14, 429-34.
- Jacquier, E., Polson, N., Rossi, P., 1994. Bayesian analysis of stochastic volatility models: Reply. *Journal of Business & Economic Statistics* 12, 413-417.
- Jacquier, E., Polson, N., Rossi, P., 2004. Bayesian analysis of stochastic volatility models with fat-tails and correlated errors. *Journal of Econometrics* 122, 185-212.
- Jeffreys, H., 1961. *The theory of probability*. Oxford University Press.

- Koopman, S.J., Lucas, A., Scharth, M., 2014. Numerically accelerated importance sampling for nonlinear non-gaussian state space models. *Journal of Business & Economic Statistics*, Forthcoming 32.
- Liesenfeld, R., Jung, R.C., 2000. Stochastic volatility models: Conditional normality versus heavy-tailed distributions. *Journal of Applied Econometrics* 15, 137-160.
- Liesenfeld, R., Richard, J., 2003. Univariate and multivariate stochastic volatility models: Estimation and diagnostics. *Journal of Empirical Finance* 10, 505-531.
- Mao, X., Ruiz, E., Veiga, H., 2013. One for all: Ecncompassing asymmetric stochastic volatility models WP, *Statistics and Econometrics* 13-11, UC3M, Spain.
- Meyer, R., Yu, J., 2000. BUGS for a Bayesian analysis of stochastic volatility models. *The Econometrics Journal* 3, 198-215.
- Nakajima, J., Omori, Y., 2012. Stochastic volatility model with leverage and asymmetrically heavy-tailed error using GH skew Students t-distribution. *Computational Statistics & Data Analysis* 56, 3690-3704.
- Omori, Y., Chib, S., Shephard, N., Nakajima, J., 2007. Stochastic volatility with leverage: Fast and efficient likelihood inference. *Journal of Econometrics* 140, 425-449.
- Richard, J.F., Zhang, W., 2007. Efficient high-dimensional importance sampling. *Journal of Econometrics* 141, 1385-1411.
- Rodríguez, M., Ruiz, E., 2012. GARCH models with leverage effect: Differences and similarities. *Journal of Financia! Econometrics* 10(4), 637-668.
- Ryzhik, I., Jeffrey, A., Zwillinger, D., 2007. Table of integrals, series and products. London: Academic Press. Seventh edition.

- Teräsvirta, T., 2009. An introduction to univariate garch models, in: Handbook of Financial Time Series. Springer, pp. 17-42.
- Tsionas, G., 2012. On generalised asymmetric stochastic volatility models. Computational Statistics & Data Analysis 56, 151-172.
- Wang, J.J., Chan, J.S., Choy, S.B., 2011. Stochastic volatility models with leverage and heavy-tailed distributions: A Bayesian approach using scale mixtures. Computational Statistics & Data Analysis 55, 852-862.
- Wang, J.J., Chan, J.S., Choy, S.B., 2013. Modelling stochastic volatility using generalized t distribution. Journal of Statistical Computation and Simulation 83, 340-354.
- Yu, J., 2005. On leverage in a stochastic volatility model. Journal of Econometrics 127, 165-178.
- Yu, J., 2012. A semiparametric stochastic volatility model. Journal of Econometrics 167, 473-482.
- Zakoian, J., 1994. Threshold heteroskedastic models. Journal of Economic Dynamics and Control 18, 931-955.